Ocean color remote sensing using polarization properties of reflected sunlight

Robert Frouin, SIO/UCSD, La Jolla, California, USA

Lydwine Gross-Colzy, CAPGEMINI, Toulouse, France

Didier Ramon, HYGEOS, Lille, France

PACE Science Team Meeting, 17-19 January 2017, Fort Pierce, Florida

CONTENTS

1. Comparison between SMART-G Monte Carlo and eGAP adding/doubling simulations of polarized radiative transfer in atmosphere-ocean system for several benchmarks.

2. Atmospheric correction using unpolarized component of top-of-atmosphere reflectance: a) Theoretical background/justification; b) PCA-based Bayesian inversion.

RT COMPARISONS

SMART-G

-SMART-G (Ramon et al., 2016) is a radiation transfer solver for the coupled ocean-atmosphere system with a wavy interface. It is based on the Monte-Carlo technique, and accounts for absorption and scattering by molecules, aerosols, and hydrosols, and Fresnel reflection/refraction at the interface.

-Polarization properties of the various atmospheric and oceanic constituents and the surface are explicitly considered. Inelastic processes (i.e., Raman scattering, fluorescence) are omitted. The ocean can be infinitely deep or bounded by a reflective bottom at finite depth. Adjacency effects can be simulated.

-The computations are made in either plane-parallel or spherical geometry. The 4 components of the Stokes vector can be obtained at any wavelength of the solar spectrum and any level of the coupled system. The vector code is written in CUDA and runs on GPU making it competitive in terms of computational speed.

RT COMPARISONS (CONT.)

SMART-G versus eGAP

-Comparisons were made between the SMART-G Monte Carlo code (plane-parallel configuration) and the eGAP adding/doubling code for several benchmarks, referred to as AOS-I*, AOS-II, and AOS-III.

-AOS-I* is the case of a molecular atmosphere with optical thickness of 0.5 (wavelength of 369.86), AOS-II is the case of a molecular ocean with a wavy surface, and AOS-III is the case of a molecular ocean and atmosphere separated by a wavy interface.

-Wind speed (to characterize surface roughness) is about 7 m/s. Wavelengths of 350, 450, 550, and 650 nm are considered for AOS-II and –III, and sun zenith angles of 30 and 60 deg.

AOS-I*, TOA

Molecular atmosphere, AOT = 0.5, SZA = 53.13°

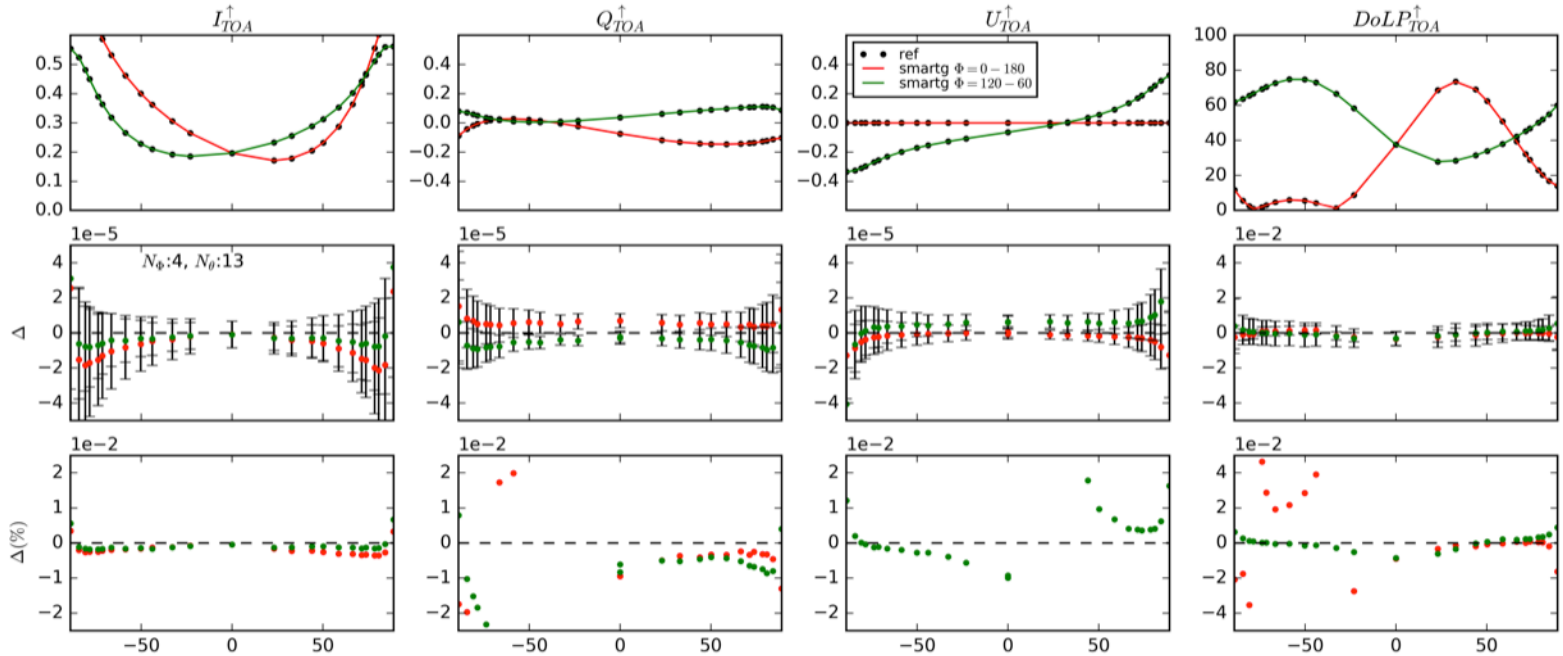

***Figure 1**: Comparison of TOA Stokes parameters (AOS-I* case, see text) computed using eGAP (ref.) and SMART-G (plane-parallel configuration) as a function of view zenith angle for relative azimuth angles of 0-180 deg. and 60-120 deg. (red and green curves). Absolute differences are <0.00004 for I, Q, and U, and relative differences are generally <0.02% for DoLP.*

AOS-II, Surface (0+)

Molecular atmosphere, wavy interface, 350 nm, SZA = 30°

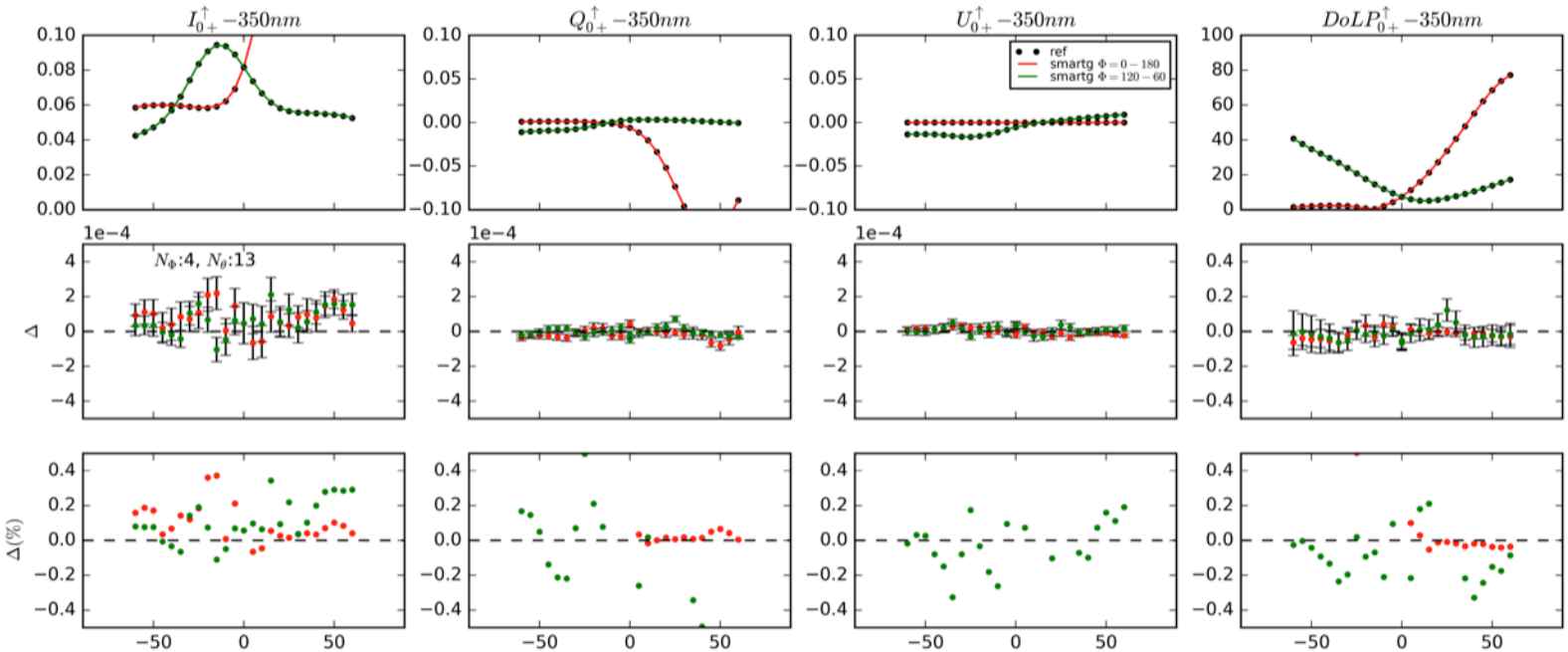

***Figure 2**: Same as Figure 1, but AOS-II case, and signal just above the surface (0+). Sun zenith angle is 30 deg. and wavelength is 350 nm. Absolute differences are <0.0002 for I, <0.00005 for Q, and U, and relative differences are generally <0.2% for DoLP.*

AOS-III, TOA

Molecular ocean/atmosphere, wavy interface, 350 nm, SZA = 30°

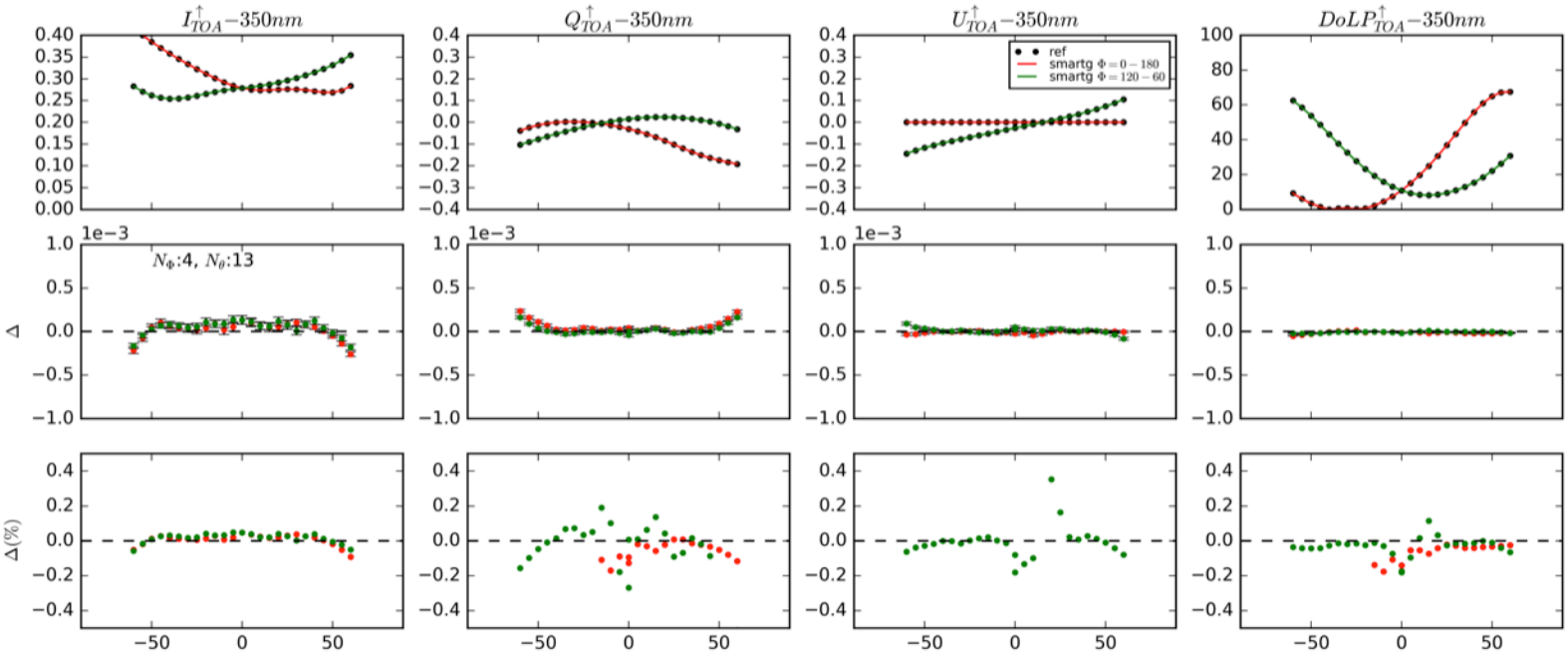

***Figure 3**: Same as Figure 1, but AOS-III case. Sun zenith angle is 30 deg. and wavelength is 350 nm. Absolute differences are mostly <0.0002 for I, < 0.0001 for Q, and U, and relative differences are <0.2% (mostly <0.1%) for DoLP.*

ATMOSPHERIC CORRECTION USING UNPOLARIZED TOA REFLECTANCE

Rationale

-A major problem in ocean color remote sensing using TOA total reflectance is that atmospheric and surface effects dominate the signal measured at the wavelengths of interest.

-To reduce these effects, one may exploit the polarization properties of reflected sunlight.

-Because molecules, hydrosols, and aerosols polarize incident sunlight, the contribution of the water body to unpolarized TOA reflectance may be enhanced, at least for some geometries.

-If the enhancement is substantial, then correction of the perturbing effects may become easier, leading to a more accurate retrieval of the water-leaving radiance (the signal to retrieve).

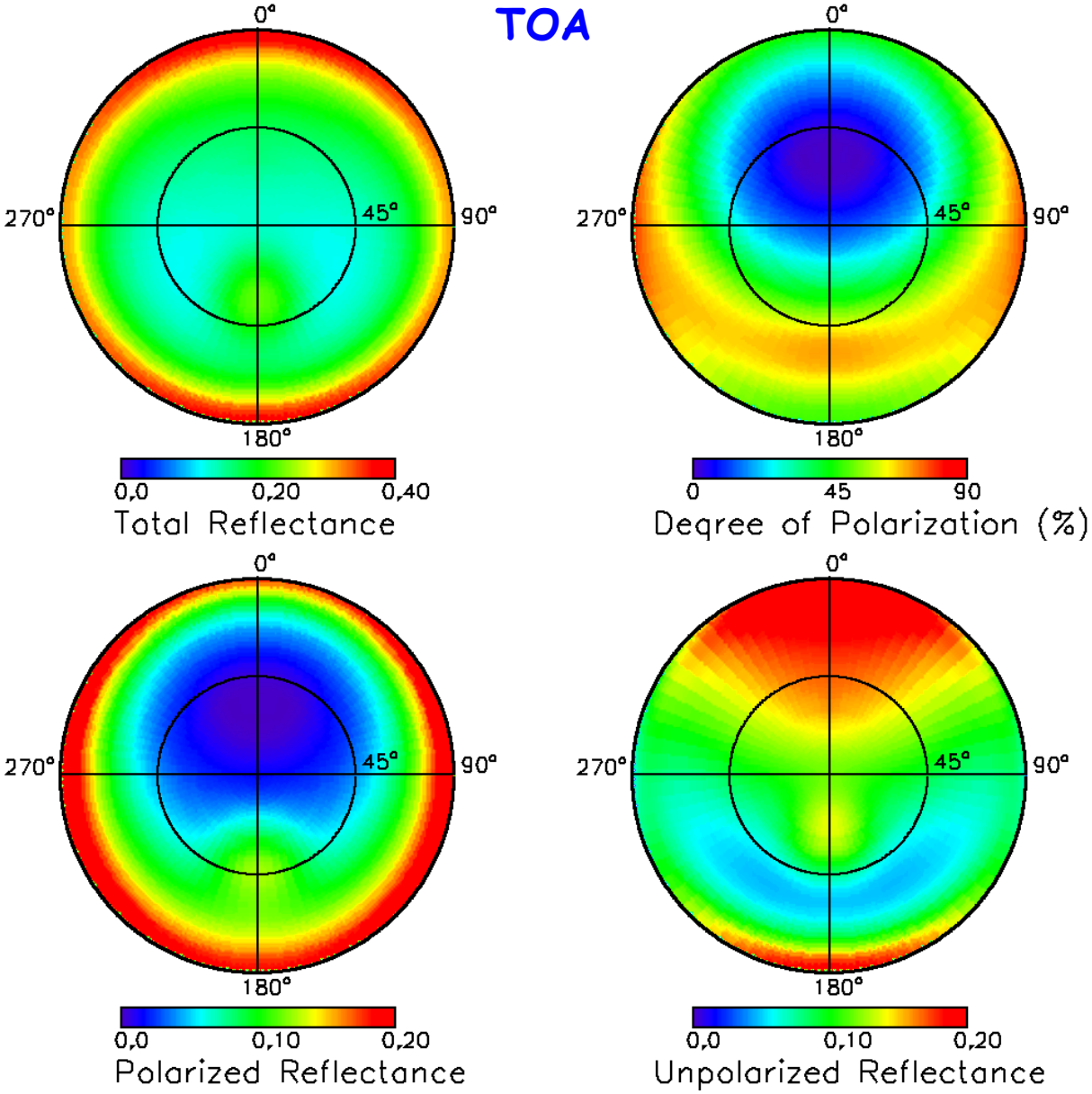

***Figure 4**: TOA total reflectance, DoLP, polarized and unpolarized reflectance ocean-atmosphere system with WMO maritime aerosols, AOT of 0.1 at 550 nm, [C 0.1 mg/m^3, and wind speed of 5 m/s. Wavelength is 443 nm, SZA of 30 deg.*

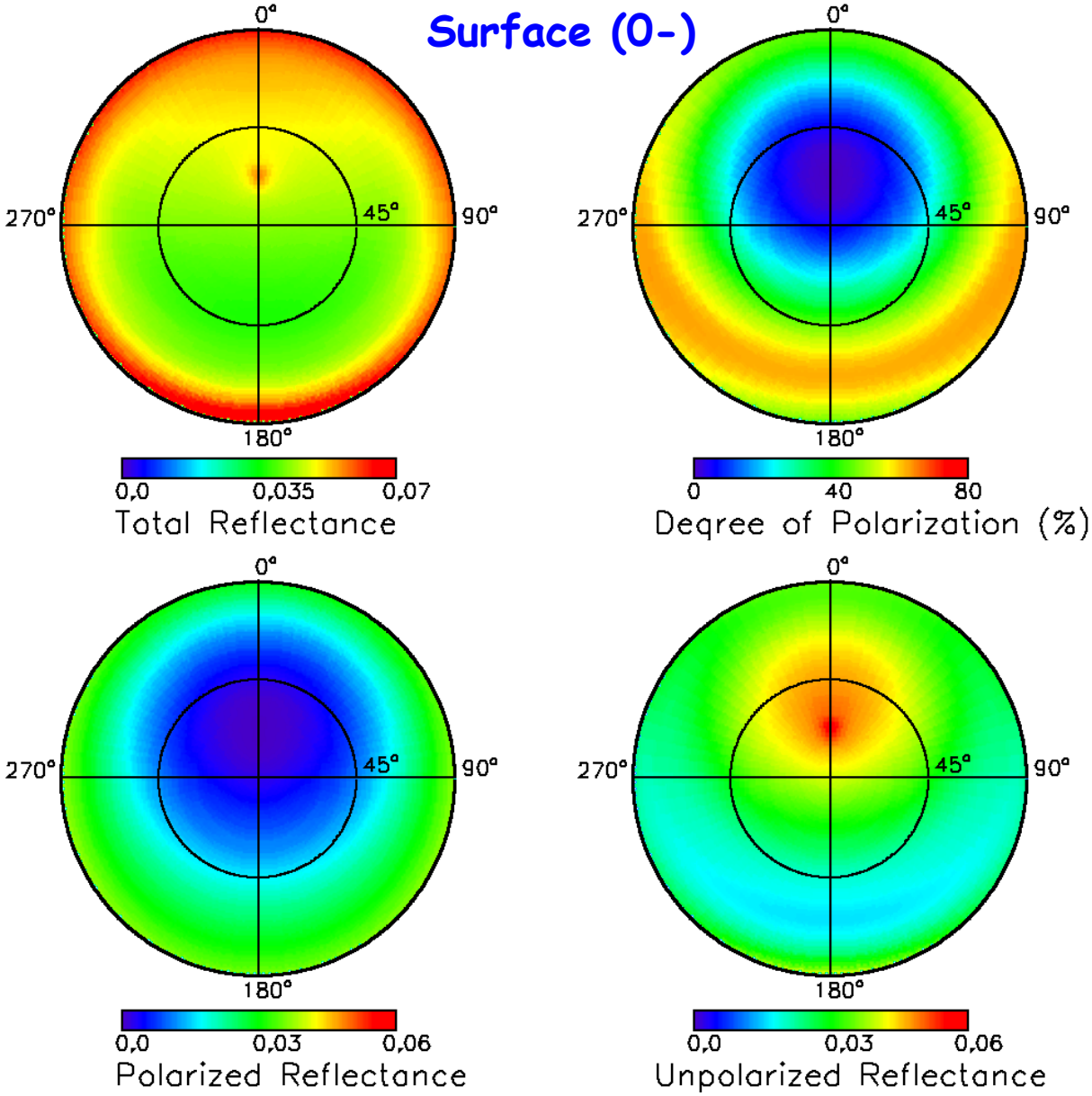

***Figure 5**: Same as Figure 4, but just below the surface (0-). Compared with T signal, no sun glint pattern, DoLP shifted due to refraction, and backward scatte peak in total and unpolarized reflectance due to hydrosol phase function.*

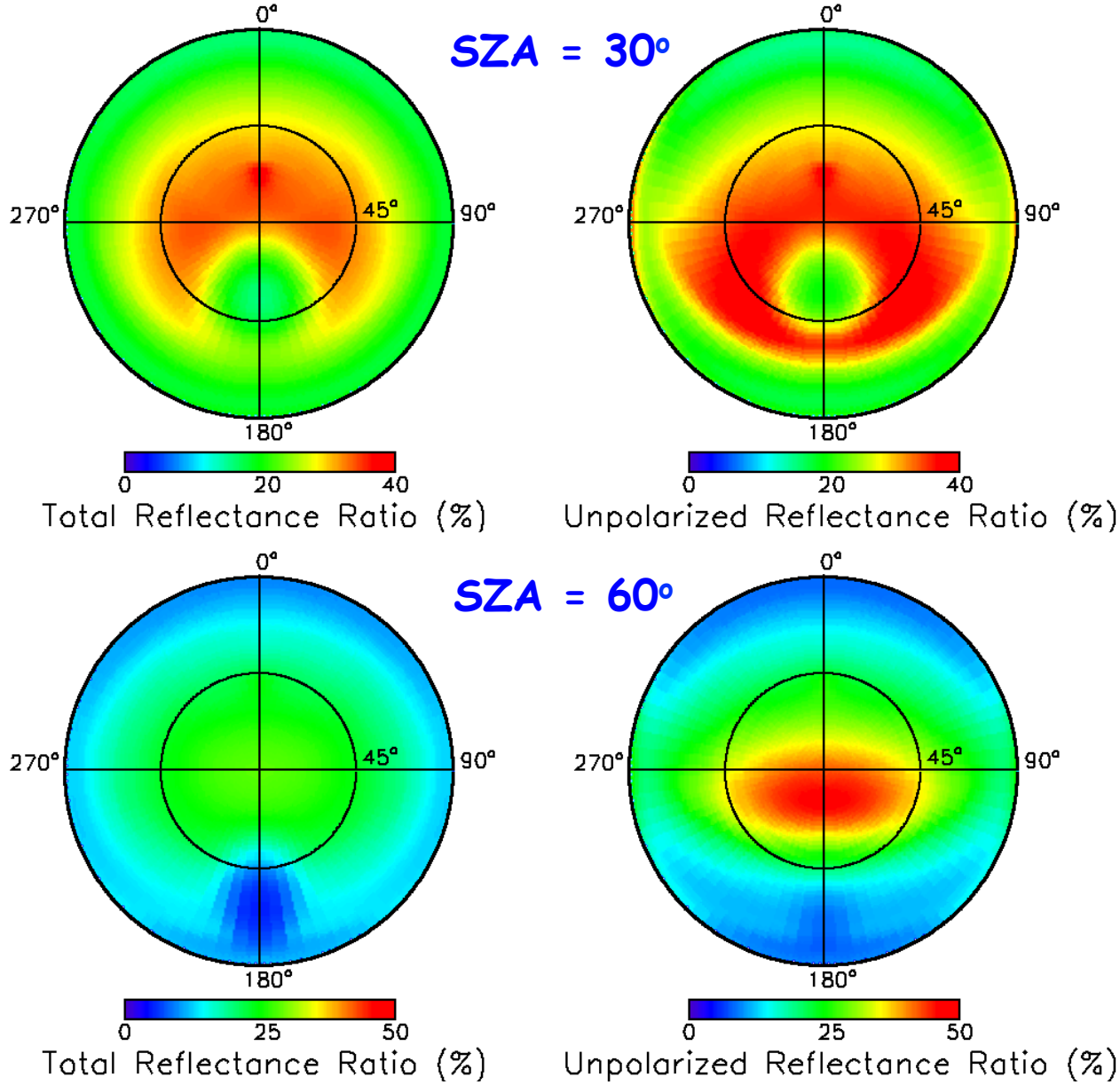

***Figure 6**: Ratios of surface (0-) and TOA reflectance, total (left) and unpolar (right). Top: SZA = 30°; Bottom: SZA = 60°. Geophysical conditions are those of Fig Ratio is generally higher for unpolarized reflectance, especially when SZA = 60°.*

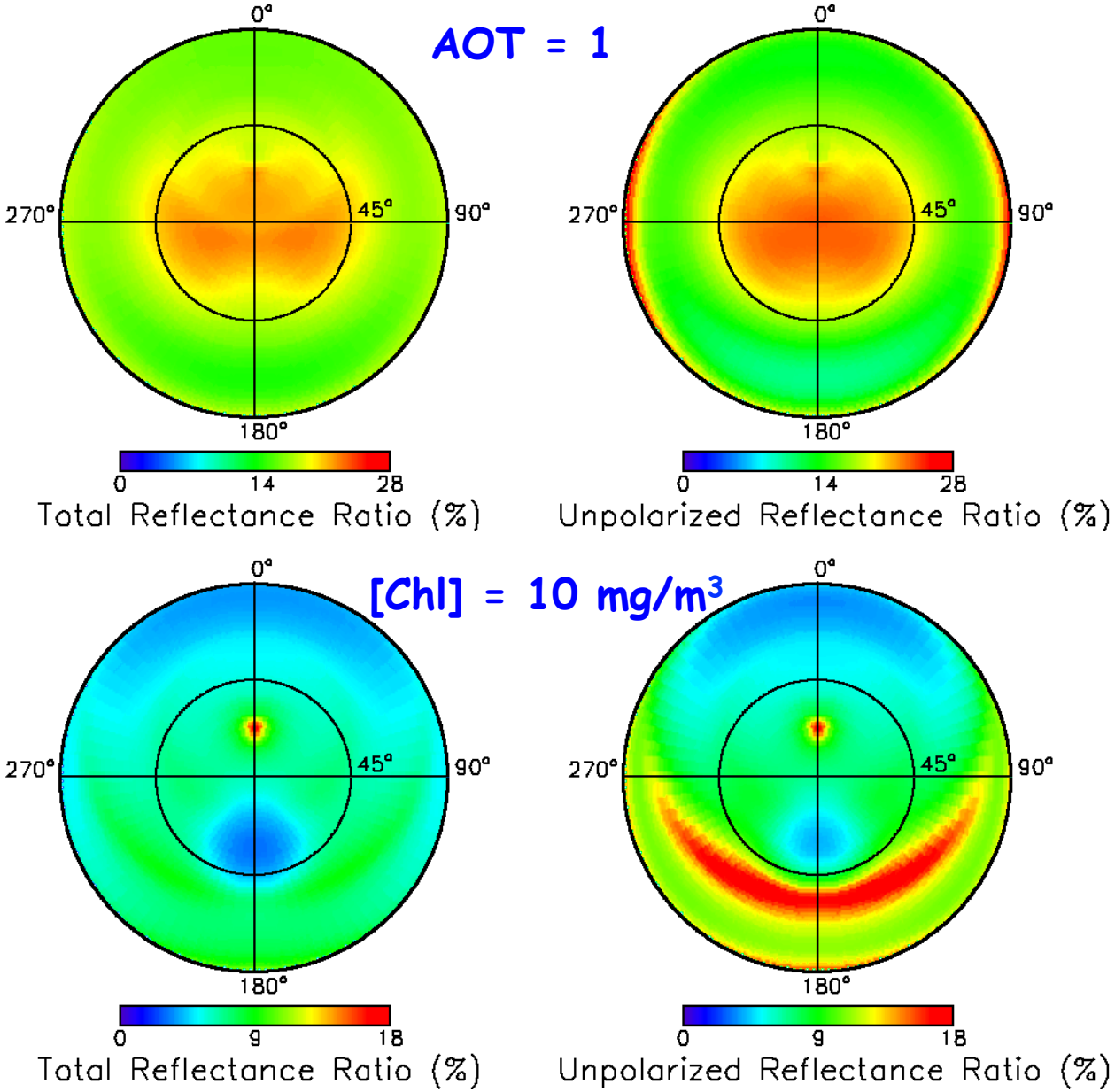

***Figure 7**: Same as Figure 6, but AOT = 1 at 550 nm (top) and [Chl} = 10 mg/m³ (bott*
No or small enhancement of the surface signal when AOT is 1, due to m
scattering, but large enhancement when [Chl] is 10 mg/m³ at scattering angles ~90 deg.

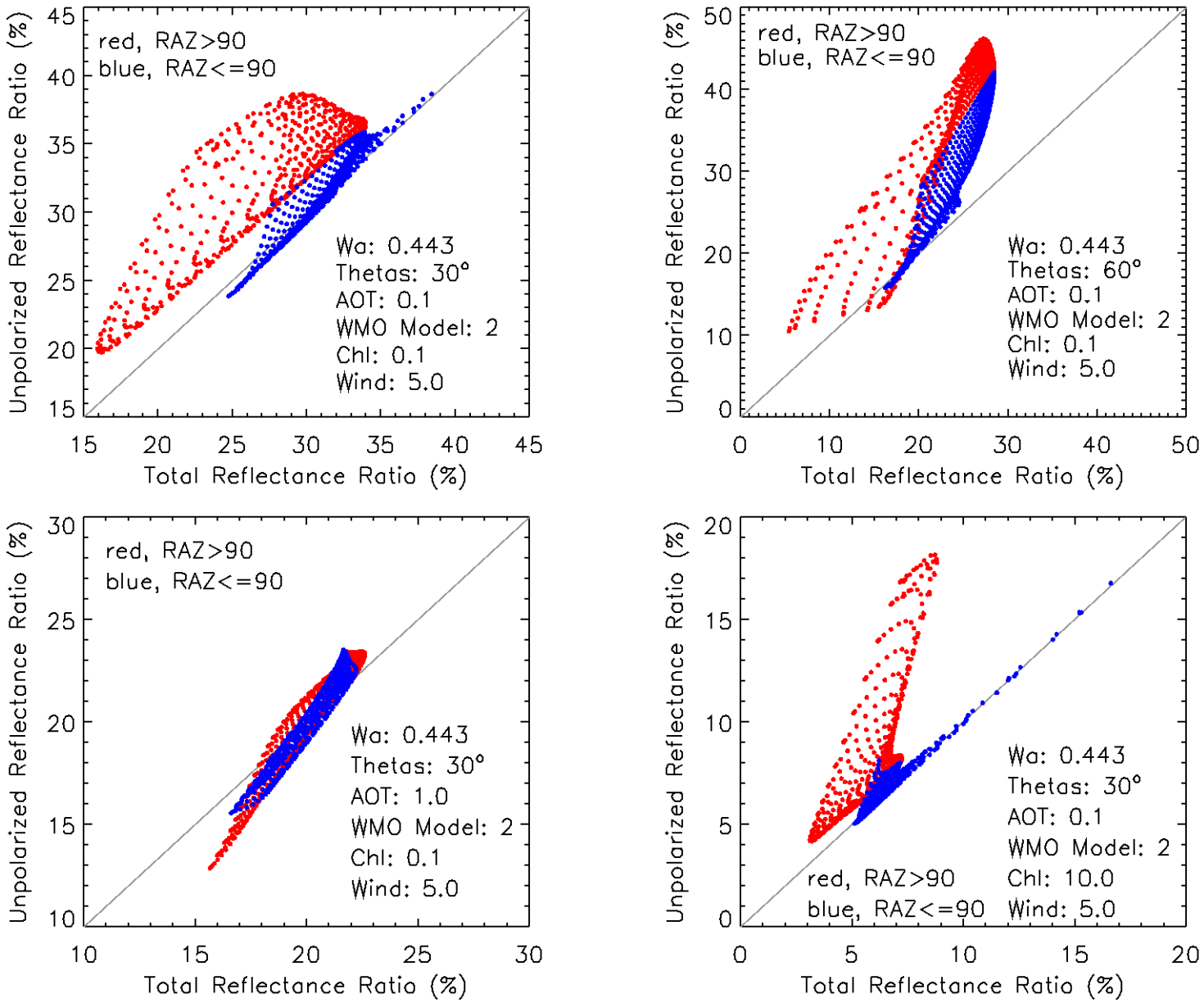

***Figure 8**: Unpolarized versus total reflectance ratio (0-/TOA) for the situatio*
Figures 6 and 7 and VZA <60 deg. Red: Forward scattering; Blue: Backward scat
Unpolarized ratio is generally higher than total ratio, except when AOT is large.

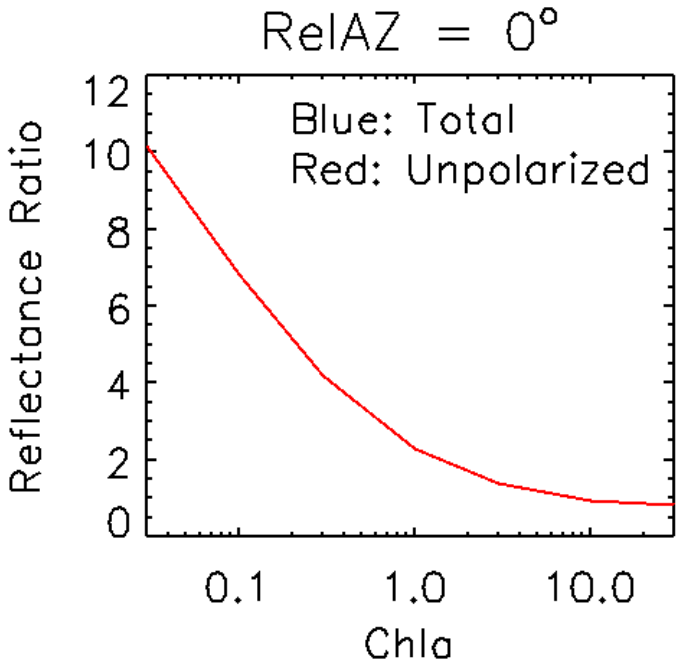

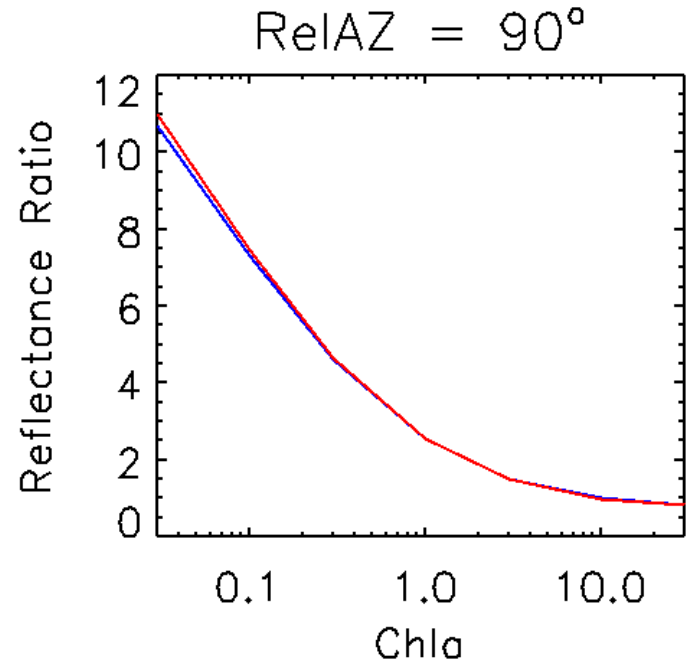

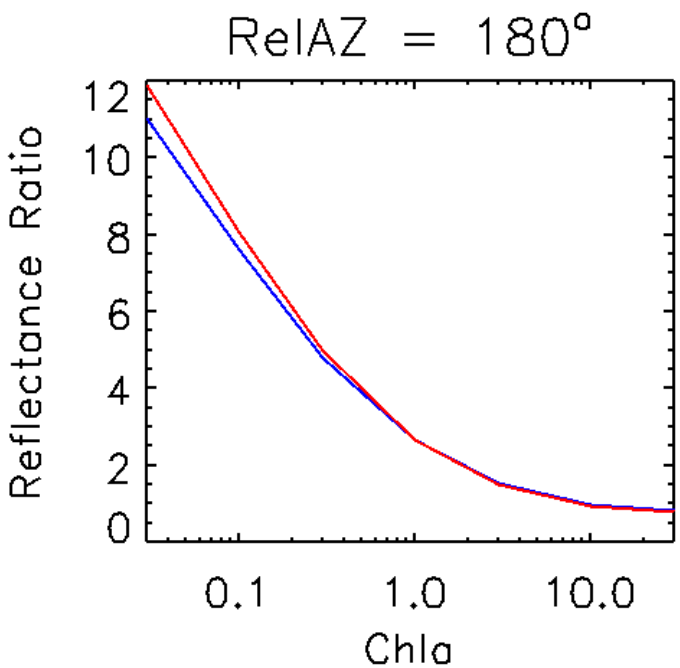

***Figure 9**: Sensitivity of ratio of water reflectance (0-) at 443 nm and 550 nm to chlorophyll concentration Chla (mg/m³). Total and unpolarized signals are used (blue and red curves). Atmospheric and surface conditions are those of Figure 1. VZA = SZA = 30°. Variation with Chla is similar using total or unpolarized reflectance.*

PCA-based Bayesian inversion

-Atmospheric correction was performed to retrieve water reflectance from unpolarized TOA reflectance in the PACE threshold aggregated bands.

-PCA-based inversion was used, in which the TOA unpolarized reflectance is decomposed into principal components, and the components sensitive to the ocean signal are combined to retrieve the principal components of water reflectance, allowing reconstruction of the water reflectance.

-The TOA signal was simulated at 350, 380, 412, 443, 490, 510, 555, 665, 748, 865, 1245, 1640, and 2135 nm for a wide range of realistic geophysical conditions and Sun and view angles. It was assumed that polarization information was available in all the spectral bands, and that the water body was not polarizing.

-Results were compared with those obtained using TOA total reflectance, to evaluate the eventual gain in retrieval accuracy when using TOA unpolarized reflectance.

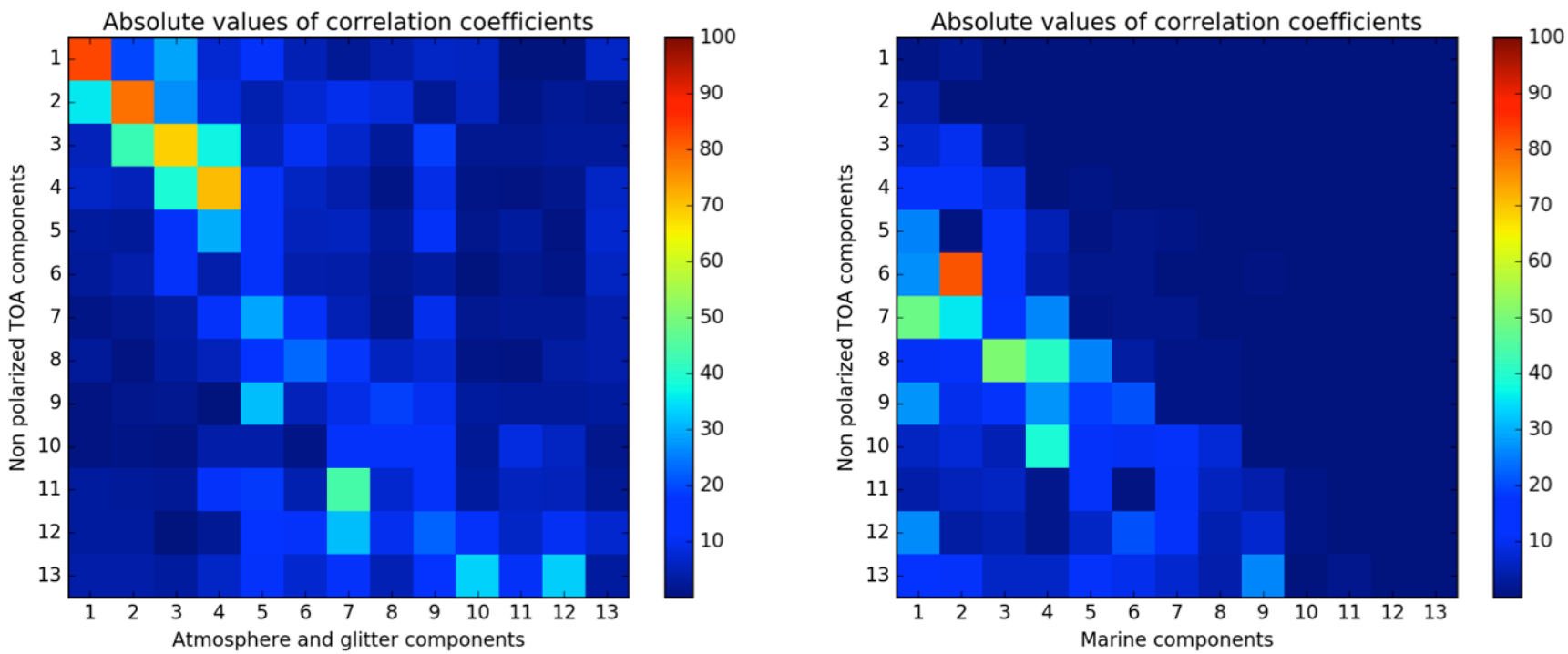

***Figure 10**: Matrices of the linear correlation coefficient (in percent) between principal components (PCs) of the TOA unpolarized signal and (left) PCs of the unpolarized atmosphere-glitter signal and (right) PCs of water reflectance, for the simulated ensembles. The first PCs of the TOA signal are strongly correlated with those of the atmosphere-glitter signal and, therefore, are not used in the mapping of water reflectance PCs, accomplished using neural network modeling.*

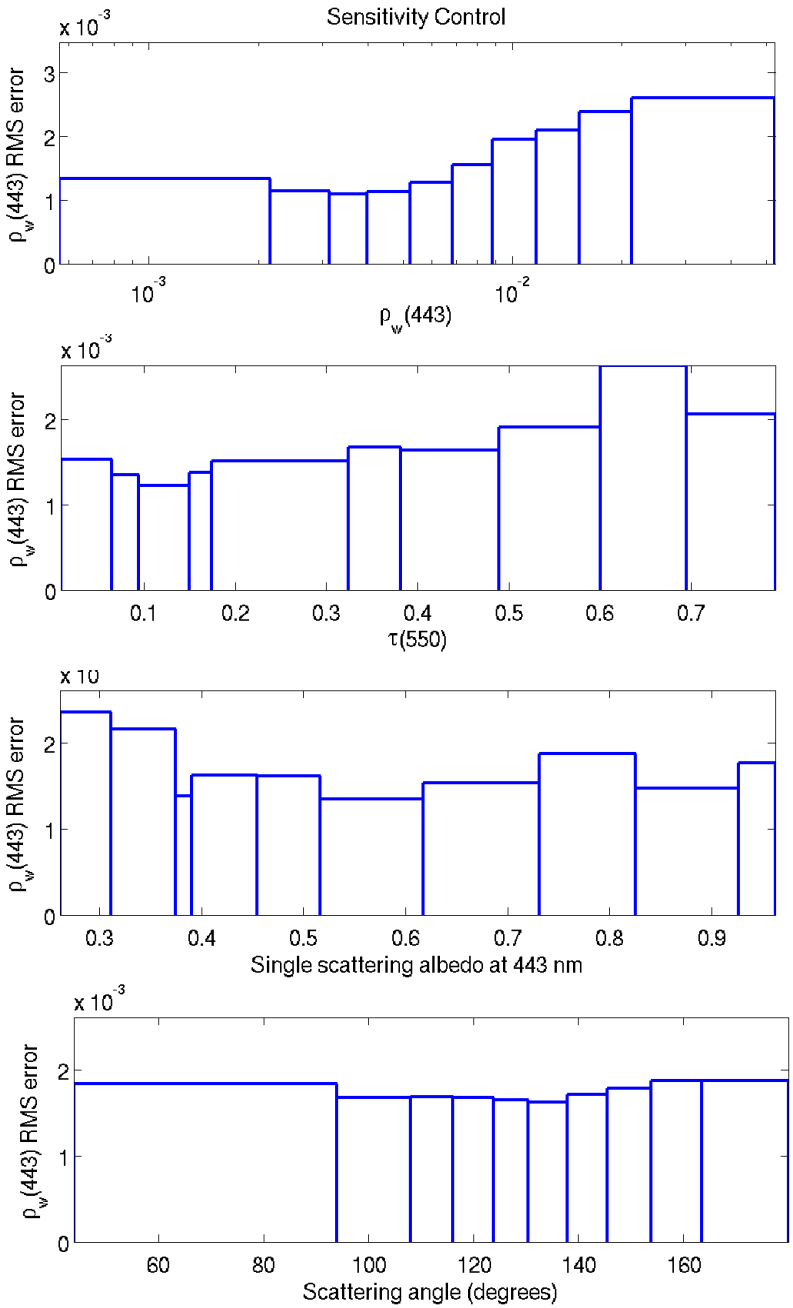

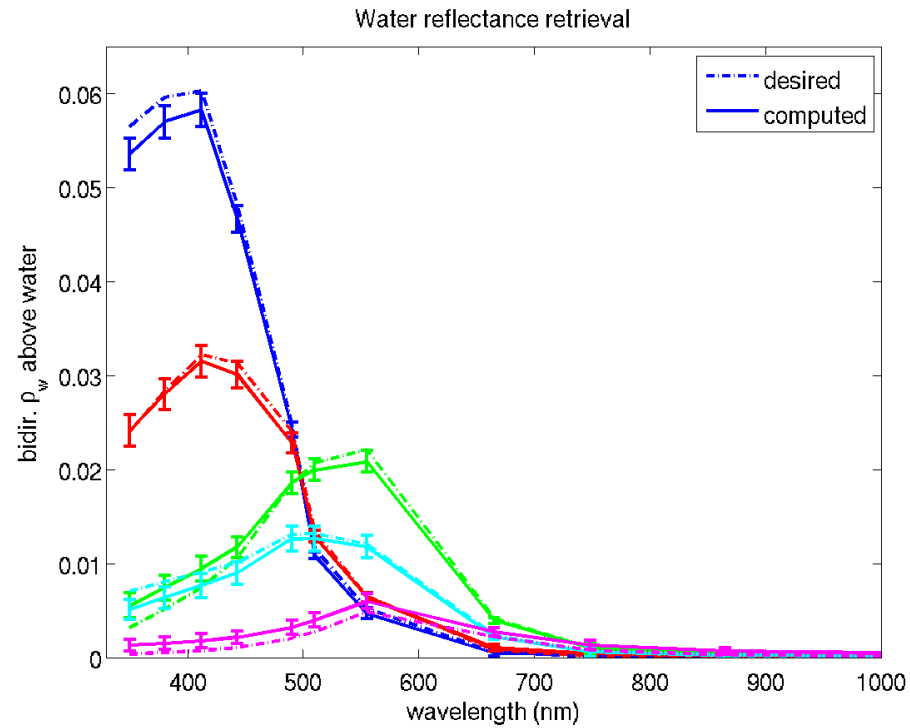

***Figure 11**: Left: Error on retrieved water reflectance at 443 nm, as a function of water reflectance, AOT, single scattering albedo, and scattering angle. The inversion is performed using the PCA-based scheme applied to TOA unpolarized reflectance in the PACE spectral bands (UV-SWIR). Top: Examples of retrieved and prescr water reflectance spectra.*

***Table 1**: Performance of the PCA-based atmospheric correction algorithm for PACE aggregated bands (UV-SWIR). Left: Using TOA total reflectance; Right: Using TOA unpolarized reflectance. RMS errors are significantly reduced using TOA unpolarized reflectance, especially in the UV and visible, e.g., by 28% at 350 nm, 36% at 443 nm, 25% at 555 nm, and 18% at 665 nm.*

	eRMS	corr(%)	bias
$\rho_w(350)$	0.00238	97	0.00022
$\rho_w(380)$	0.00248	97	0.00029
$\rho_w(412)$	0.00236	98	0.00031
$\rho_w(443)$	0.00204	98	0.00026
$\rho_w(490)$	0.00186	96	0.00020
$\rho_w(510)$	0.00165	93	0.00014
$\rho_w(555)$	0.00158	93	0.00011
$\rho_w(665)$	0.00068	96	0.00007
$\rho_w(748)$	0.00073	96	0.00005
$\rho_w(865)$	0.00043	97	0.00001
$\rho_w(1245)$	0.00006	95	-0.00000

(Total)

	eRMS	corr(%)	bias
$\rho_w(350)$	0.00171	98	0.00009
$\rho_w(380)$	0.00162	98	0.00012
$\rho_w(412)$	0.00154	99	0.00014
$\rho_w(443)$	0.00130	99	0.00010
$\rho_w(490)$	0.00126	98	0.00009
$\rho_w(510)$	0.00121	96	0.00006
$\rho_w(555)$	0.00119	96	0.00005
$\rho_w(665)$	0.00056	97	0.00003
$\rho_w(748)$	0.00070	99	0.00012
$\rho_w(865)$	0.00041	99	0.00006
$\rho_w(1245)$	0.00002	100	-0.00000

(Unpolarized)

CONCLUSIONS

-Agreement is very good between SMART-G Monte Carlo and eGAP adding/doubling RT simulations for benchmarks AOS-I*, AOS-II, and -III, generally to a small fraction of one percent for both I and DoLP (better for AOS-I*, the case of a molecular atmosphere).

-Using unpolarized reflectance instead of total reflectance, the contribution of the water body to the TOA signal is generally enhanced, except over optically thick atmospheres (due to multiple scattering), making the atmospheric correction easier. Sun glint is not an issue anymore, and determination of the aerosol model is facilitated by using polarization information in addition to spectral information in the NIR-SWIR. Sensitivity of the unpolarized water reflectance to chlorophyll concentration is adequate.

-PCA-based atmospheric correction applied to simulated PACE data in the aggregated bands indicates significant improvement in water reflectance retrievals when working with TOA unpolarized reflectance, with RMS errors reduced by 28% at 350 nm, 36% at 443 nm, 25% at 550 nm, and 18% at 665 nm.